Nat Hazards (2017) 88:389–414
DOI 10.1007/s11069-017-2871-x

ORIGINAL PAPER

Mapping the coastal risk for the next century, including sea level rise and changes in the coastline: application to Charlestown RI, USA

Annette Grilli[1] · Malcolm L. Spaulding[1] · Bryan A. Oakley[2] · Chris Damon[3]

Received: 28 November 2016 / Accepted: 9 April 2017 / Published online: 19 April 2017

Abstract A source–pathway-receptor method is used to assess the risk of the coastal community of Charlestown, RI, USA, to the 100-year storm, including effects of sea level rise (SLR) and shoreline/dune erosion. The 100-year storm is simulated using a chain of stochastic and physics-based models combined with a scenario-based approach. Storm surge and wave spectral parameters, obtained from the U.S. Army Corps of Engineers' North Atlantic Coast Comprehensive Study (NACCS), are used as boundary conditions for high-resolution wave simulations, performed in the coastal and inundation zones using the steady-state spectral wave model STWAVE. Selected scenarios are defined to assess the magnitude of the variability in predicted damage resulting from the uncertainty in SLR, erosion rate, and time at which the 100-year storm would occur. Erosion rates are based on empirical analyses of historic rates of shoreline change, SLR measurements, and coastal erosion theory. The risk is measured in terms of damage to individual houses, based on damage curves developed in the U.S. Army Corps of Engineers, NACCS study. In addition, remediation scenarios are explored, demonstrating that a combination of dune replenishment and an increase in the residential resilience by elevating structures can significantly diminish the risk to the coastal community.

✉ Annette Grilli
agrilli@egr.uri.edu

Malcolm L. Spaulding
spaulding@egr.uri.edu

Bryan A. Oakley
oakleyb@easternct.edu

Chris Damon
cdamon@edc.uri.edu

[1] Ocean Engineering, University of RI, Narragansett, RI, USA

[2] Eastern Connecticut State University, Willimantic, CT, USA

[3] Environmental Data Center, University of RI, Kingston, RI, USA

Keywords Damage to coastal structures · Inundation · Flooding · Wave · Sea level rise · Coastal erosion · Dune erosion

1 Introduction

The alarming sea level rise (SLR) projections over the next century combined with the predicted increase in the frequency of strong storms (Bender et al. 2010) call for a re-evaluation of current flooding maps. This task is complicated due to the large uncertainty inherent in such projections, resulting from the complexity of the processes involved, as well as assumptions on which the models used to generate the estimates are based. This uncertainty propagates, through the modeling chain, to the inundation maps. Transparency about this uncertainty is sought, suggesting either a probabilistic framework of the coastal risk that local communities are exposed to, or a scenario-based approach to the risk, or a combination of both (e.g., Probabilistic Coastal Flood Hazard Analysis and Mapping for the USA, May 15, 2015, workshop at The Rockefeller Foundation, NY).

In recent work, we developed and applied a methodology for estimating the structural risk that individual coastal houses face in storm events, using a combination of a probabilistic approach to simulate the 100-year storm parameters, physics-based approaches to simulate storm surge and wave propagation, and a scenario-based approach to simulate different SLR scenarios (Spaulding et al. 2016). The damage curves proposed by the US Corps of Engineers (Simm et al. 2015) were used to relate the environmental hazard from surge and waves to the structural risk, at the scale of individual houses. This approach was the basis for the development of a Coastal Environmental Risk Index (CERI) recently applied to select Rhode Island (RI) coastal communities (Spaulding et al. 2016).

In this study, we similarly combine probabilistic, physics-based and scenario-based approaches to assess the risk faced by the coastal community of Charlestown, RI, but we expand the methodology to include changes in the coastline associated with SLR. The selected scenarios attempt to quantify the variability resulting from the uncertainty in SLR, erosion rate, and time at which the 100-year storm would occur. A 100-year return period event is an event with a probability of occurrence of 1% every year, and it can therefore happen any time. We assess the variability of the impact of the 100-year storm as a function of its time of occurrence, by modeling the 100-year storm for two equally likely scenarios: tomorrow or in 2100. For each scenario, the storm propagates on different mean sea level (MSL) due to SLR and faces a different morphology of the coastline due to the associated erosion. Erosion rates are based on empirical analyses of historic shoreline change (with sampling representative of the geological characteristics of the area), SLR measurements, and coastal erosion theory.

In addition, we explore remediation scenarios designed to decrease the risk faced by the coastal community. Two approaches are considered: increasing the resilience of the community or altering the storm pathway to reduce the impact of the storm on the community.

It is convenient to recast our proposed approach in the source–pathway–receptor (SPR) conceptual framework (Oumeraci 2004, 2005, 2015), as shown in Fig. 1. The *source* in this work is expressed in terms of stochastic events, e.g., the 100-year storm, the *pathway* is provided in terms of dune state (intact and eroded) and SLR, and the resulting impact is assessed on the *receptors*, i.e., the individual houses in the area of interest, in terms of the

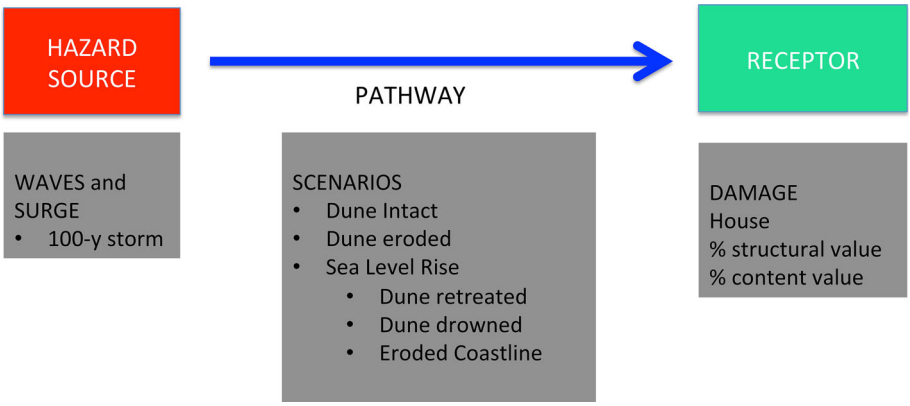

Fig. 1 Source–pathway–receptor conceptual framework (SPR) as used in the to the CERI project (based on and modified from Oumeraci 2004)

relative (%) structural damage. Different scenarios can be simulated by modifying the *source*, the *pathway,* or the *receptors,* independently, or simultaneously.

The SPR approach was extensively used in the interdisciplinary European project "XtremRisK," an integrated flood risk analysis for extreme storm surges at open coasts and in estuaries (e.g., Burzel et al. 2015; Oumeraci et al. 2015; Naulin et al. 2015). Its use was extended worldwide, establishing this concept as a standard reference framework to assess the coastal impact of extreme storms (e.g., Cui et al. 2015, Narayan et al. 2015, Yan et al. 2016).

1.1 Hazard source

The hazard source is assessed in terms of storm surge and wave impact at the coast. While the U.S. National Oceanic and Atmospheric Administration (NOAA) routinely uses surge and wave models to simulate storms in real time providing fast estimates of storm surge, other modeling teams have focused on improving long-term predictions by relating typical storms to a return period. Emanuel et al. (2006, 2008, 2013) developed a *statistical-deterministic* approach to deterministically generate synthetic storms with physics-based models, with the storm environments statistically defined. Lin et al. (2012) extended the method to a *dynamical-statistical* approach simulating synthetic storms associated with climate model simulations to account for future storm climatology changes. Lin and Emanuel (2016) applied their dynamical-statistical approach to assess the storm surge risk on specific coastal communities.

Other teams recently used similar statistical-deterministic approaches at local or regional scales. In the context of the North Atlantic Coast Comprehensive Study (NACCS), the U.S. Army Corps of Engineers (USACE) generated synthetic tropical and historical extratropical storms, simulating surge and waves using the fully coupled surge (ADCIRC) and phase-averaged steady-state spectral wave (STWAVE) models (Smith et al. 2001; Massey et al. 2011; Anderson and McKee-Smith 2015). NACCS provides storm surge and wave spectral parameters at many *save points*, in a probabilistic form (return period) (Cialone et al. 2015; Nadal-Caraballo et al. 2015). Addressing the difficulty of accurately modeling inundation in complex sites, Orton et al. (2016) focused on the New York Harbor inundation risk. They used a statistical-deterministic approach to accurately model storm

tides for return periods of 5–10,000 years, after performing a careful calibration with historical storms.

Bilskie et al. (2014) extended the paradigm of simulating storm surge in the near future by integrating alterations of the current landscape resulting from SLR, using the tightly coupled Simulating WAves Nearshore (SWAN) and the ADvanced CIRCulation (ADCIRC) models (Luettich et al. 1992; Dietrich et al. 2011). The approach was recently refined (Bilskie et al. 2016) by the inclusion of a biomass-corrected topographic elevation (Medeiros et al. 2015). Passeri et al. (2015, 2016) studied the sensitivity of the hydrodynamic response to the inclusion of long-term shoreline changes along the Northern Gulf of Mexico shoreline (Alabama/Florida).

In this work we use a statistical-deterministic approach to model storm surge at the regional scale, combined with a deterministic wave modeling at the local scale, using the NACCS statistical spectral parameters generated at the save points to force a local wave model. In addition to the storm surge, that is often solely used to assess the inundation risk, we include effects of wave propagation in the inundation zone (Grilli et al. 2015). We also extend the paradigm of storm surge simulation in the future by integrating changes in the coastline, in particular, the dune barrier retreat.

1.2 SLR scenarios

The most recent estimates of historical global mean sea level (GMSL), which are based on a statistical analysis of collected data at gauges, yield a global SLR rate of 3.0 ± 0.7 mm per year, between 1993 and 2010 (Hay et al. 2015). This value is significantly larger than the general trend observed during the last century (1900–2009: 1.6–1.9 mm per year; Church and White 2011), confirming the observed acceleration in SLR that has been reported in the past 10 years, based on satellite data (3.2 ± 0.4 mm per year) or in situ data (2.8 ± 0.8 mm per year), recorded between 1993 and 2009 (Church and White 2006, 2011). In parallel with this recent revision of the historical GMSL, improvements in the understanding and modeling of land–ice interactions has allowed expanding the physics incorporated in process-based models, beyond the traditional thermal expansion of the ocean and the melting of glaciers, providing updated SLR projections (Levermann et al. 2013). These models, however, have a very large uncertainty associated in part with the complex nonlinearity of the processes involved, resulting in large confidence intervals for any future SLR projection.

Besides the uncertainty associated with physical processes, SLR projections also have an uncertainty associated with CO_2 emissions. The Intergovernmental Panel on Climate Change (IPCC) has defined several Representative Concentration Pathway (RCP) scenarios, each representing a specific pattern in future CO_2 emission. The IPCC Fifth Assessment Report (AR5; 2014) published several SLR projections based on four RCP scenarios and process-based models (Church et al. 2013). The RCP scenarios are named after the value of their radiative forcing in 2100, relative to pre-industrial values (e.g., +2.6 and +8.5 W/m^2, for the extreme scenarios RCP2.6 and RCP8.5, respectively) (Weyant et al. 2009; Moss et al. 2010). The currently measured CO_2 emission closely follows the worst-case scenario, RCP 8.5, and thus leads to the largest forecast temperature increase in 2100, providing a *likely* expected global averaged SLR in 2100 between 0.5 and 1 m above the 1986–2005 level. Expected *likely* SLR following an ideal best-case scenario (immediate reduction of CO_2 emission) is in the range of 0.3–0.6 m by 2100. Results in the AR5 are provided with two measures of uncertainty: the aleatory uncertainty, a quantified measure of uncertainty expressed probabilistically based on statistical analysis of model

results, and the epistemic uncertainty, a qualitative measure of uncertainty, expressing the confidence in the results based on the quality of the models (e.g., understanding the processes), consistency of evidence, and degree of agreement among experts. The cited *likely* range represents a probability in the 66–100% likelihood range; these projections are combined with a *medium* confidence (Peters et al. 2013; Church et al. 2013).

Federal agencies, NOAA (Parris et al. 2012) and USACE (USACE 2011), have published SLR projections based initially on a methodology developed in 1987 by the National Research Council (National Research Council 1987; Gornitz et al. 1982), and more recently updated following the IPCC Fourth Assessment Reports (AR4 2007). The current parameters for Newport, RI, are listed in Table 1 and are combined in Eq. (1) to estimate the SLR (ΔS) in any given year t_2 relative to a reference year (t_1) as,

$$\Delta S = M(t_2 - t_1) + b\left(t_2^2 - t_1^2\right) \tag{1}$$

where M is the regional SLR rate (m/year), equal to the sum of the eustatic (ESL) and the local vertical movement (LVM), as estimated in 1992 (mid-year of current National Tidal Datum Epoch, 1983–2001) and b is a parameter defining the curvature of the projection. These provide a mid-range of *intermediate low and high* projection by 2100 of 0.6 m and 1.3 m, respectively, with *low* and *high* limits of 0.3 and 2.1 m, respectively. Projections used by the USACE are identical for the lowest scenarios but more optimistic for the worst-case scenario, providing a maximum expected SLR in 2100 of 1.6 m (Zervas et al. 2013; Hubert and White 2015).

Horton et al. (2014) developed an *expert elicitation* survey, as an attempt to enlighten the uncertainty in predicting the magnitude of SLR. Most experts (135 participated) provided SLR estimates by 2100 consistent with the upper confidence interval of the likely values presented in the IPCC AR5 projects, and with the NOAA intermediate scenarios. Experts would cite as the most likely low (RCP 2.6) and upper temperature (RCP8.5) scenarios by 2100, a 0.4–0.6 m, and a 0.7–1 m SLR, respectively. Thirteen experts ($\sim$10%) estimated a 17% probability of exceeding 2.0 m of SLR by 2100, under the upper temperature scenario (RCP8.5). Pfeffer et al. (2008), in particular, included the possibility and related physics for a rapid melting of the ice sheets and found a high scenario similar to NOAA's highest scenario. An extensive review of SLR projection is provided by Nicholls et al. (2014).

In our scenarios, we have tried to account for the large uncertainty in SLR projection by selecting two scenarios representative of the most likely best- and worst-case scenarios.

We selected 0.6 m as our most likely best scenario. This scenario corresponds to the NOAA intermediate low scenario at Newport, to the upper bound of RCP 2.6 and the lower bound of the RCP8.5. Our worst-case scenario corresponds to the NOAA highest scenario

Table 1 Parameters to estimate NOAA and USACE SLR scenarios in Newport, RI (#8452660), including eustatic (ESL) and local vertical movement (LVM), as defined in Eq. (1)

Scenario	Parameters					
	b				M	
	Low	Intermediate low	Intermediate high	Highest	ESL (m/year)	LVM (m/year)
USACE	0	0.0000271		0.00013	0.0017	0.0009
NOAA	0	0.0000271	0.0000871	0.000156	0.0017	0.0009

at Newport (Table 1), and to the most extreme scenarios designed by experts. These are referred to in the following as the 2-*foot* (2-ft) and 7-*foot* (7-ft) scenarios. The 2-ft scenario constitutes our lower bound, associated with a high certainty, while the 7-ft case is our worst-case scenario, associated with a low certainty but providing an upper bound of safety necessary for policy management.

1.3 Erosion

As sea level rises, beaches are eroded and the shoreline recesses inland provided space is available to do so. Indeed, when the water level changes, the beach profile adjusts to maintain an equilibrium beach profile resulting from a balance between destructive and constructive forces (Dean and Dalrymple 2004). The concept of the equilibrium beach profile makes it therefore possible to estimate the beach response to a change in the forcing, such as SLR. Bruun (1962, 1988) was the first to propose a relationship (the Bruun rule), defining the equilibrium profile response (R) to an increase in sea level (S), as the ratio of S to the average beach slope over the active beach profile, γ $\left[R = \frac{S}{\gamma}\right]$. The original Bruun's law, often largely criticized for its simplified assumptions (e.g., Cooper and Pilkey 2004), was subsequently revisited, in particular for the case of a barrier island (e.g., Godfrey and Godfrey 1973), leading to the generalized Bruun's law (Dean and Maurmeyer 1983; Dean 1991; Rosati et al. 2013).

Among the coastal resilience studies including shoreline geomorphological changes associated with SLR into hydrodynamic modeling, Reece et al. (2013) used Bruun's rule to estimate the shoreline erosion for selected SLR values based on an expected SLR of 1 m by 2100. More recently, Passeri et al. (2015) estimated the 2050 Gulf shoreline by extrapolating the historic shoreline rate of change based on the National Assessment of Coastal Vulnerability to SLR data base (CVDB; Thieler and Hammar-Klose 2000; Pendleton et al. 2010). In agreement with the equilibrium beach profile theory, the current beach profile of the Northern Gulf coastline in Passeri et al. (2015) is assumed translated upward by the amount of SLR, and landward or seaward by the amount of projected erosion or accretion while maintaining its shape. Passeri et al. (2016) and Plant et al. (2016) used a Bayesian network (Gutierrez et al. 2011, 2014) to make probabilistic assessments of shoreline changes associated with SLR to address the complexity of predicting future coastline changes at a large scale.

In this analysis, we assume a linear relationship between SLR and erosion rate based on equilibrium beach profile theory. However, we use the historical rate of shoreline change (erosion) and measured rate of SLR, which allows us to avoid some of the criticisms of Bruun's law. We implicitly integrate all the physical processes associated with erosion, including the increase in storm frequency, as discussed in the next section.

1.4 Risk

While the hazard for each house located near the coastal feature is assessed in terms of the 100-year inundation depth and maximum wave crest elevation (1% probability of exceedance), the vulnerability of each house is essentially based on its first floor elevation, as well as the house type, as defined by the USACE (Simm et al. 2015). The risk is theoretically defined as the product of the hazard and structural failure probabilities. In this analysis, since the hazard probability is a priori specified as a constant 1% value, the risk is simply proportional to the probability of structural failure. In our analyses, we use the

maximum expected structural damage (%; relative to the value of the structure) that each house would face, if subject to the 1% event, as a variable to assess the risk. The relative damage is assessed using the USACE damage curves, which provide the expected relative damage as a function of inundation depth and maximum wave crest elevation. The risk is currently restricted to residential structural damage, but the method is readily extendable to infrastructure (e.g., fire stations, schools, hospitals, etc.) and associated services (e.g., access to escape roads, access to fire stations, access to hospitals).

1.5 Study area, Charlestown, RI

The study area (Fig. 2) is located on the southern shore of RI, USA, and is protected by two barrier beaches from predominantly southerly waves travelling through Block Island and RI sounds. While the offshore average significant wave height is around 1.2 m, the expected 100-year offshore significant wave height is on the order of 10 m (Wave Information Studies, WIS). Although the mean tidal range is about 1 m (NOAA station 8452660), the maximum storm surge observed (New England Hurricane 1938) was on the order of 5 m above MSL (Holman and Sallenger 1985). The heart of the Charlestown community is settled on the Northern shore of Ninigret pond in a flat area, mostly below 7 m, as well as on the headland between the two ponds, Ninigret and Quonochontaug. The headland is formed of glacial till creating a relatively higher point, up to 8 m, compared to the adjacent barrier beaches' elevation, which varies between 3.5 and 4.2 m. The Ninigret beach barrier is about 300 m wide and is mostly vegetated with low bushes and pine trees,

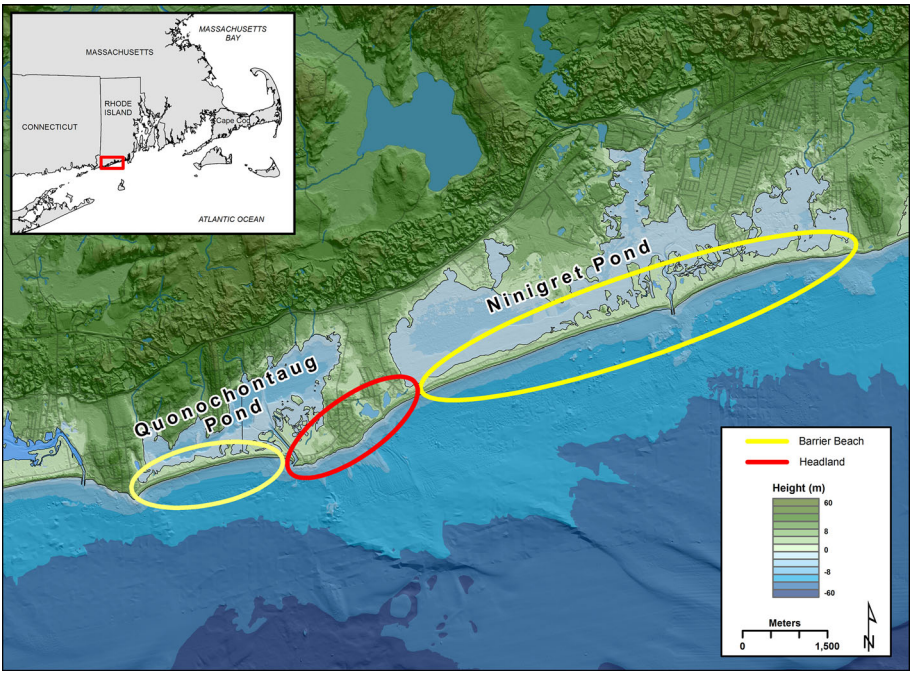

Fig. 2 Study area showing the dune barrier and headland systems in Charlestown, RI.; barrier in *yellow*; headland in *red*. Bathymetry/topography in background

although it is also partially developed with houses expanding on its extreme east and west sides.

In the following, we first detail the methodology for performing dynamical scenario-based analyses, with a focus on estimating wave propagation and coastal impact during a 100-year storm with a modified coastline. Wave simulations are performed using the phase-averaged wave model STWAVE and flood inundation based on the statistical-deterministic approach provided by the NACCS study. We then present results of high-resolution (10-m) nearshore simulations for selected scenarios of the 100-year storm occurring between today and 2100, along the southern RI coast. Simulations are performed for the two selected SLR scenarios, 2 and 7 ft, and for hypothetical natural erosion scenarios as well for proposed remediation scenarios, both described in the next section. Future shoreline erosion is assessed using extensive historical shoreline transect data and geological characteristic of the coast (Oakley 2016), combined with shoreline erosion theory (Dean and Dalrymple 2004).

2 Methodology

We apply a scenario-based methodology, following the SPR concept (Fig. 1). Each component is described in detail in the following.

2.1 Hazard source

The hazard source consists of storm surge, combined with tides, and waves. The prototype 100-year storm is designed using the NACCS statistical outputs, surge (including astronomical tide and static wave setup) and spectral 100-year parameters at the local save points, as offshore boundary conditions to the high-resolution (10 m) nearshore wave simulations using STWAVE. Mean values of the wave spectral parameters, significant wave height (H_s), and peak wave period (T_p) were extracted from the NACCS save points and interpolated along the offshore boundary of the nested grid to reconstruct the local spectrum assuming a TMA shallow-water spectrum (Bouws et al. 1985). Waves are propagated on the static water level (STWL) combining the astronomical tide, storm surge, and static wave setup. The bottom friction is specified using a spatially variable Manning friction coefficient, related to land coverage (Wamsley et al. 2009; RIGIS 2013). Grid characteristics and spectral boundary conditions are summarized in Tables 2 and 3, respectively.

STWAVE was applied in half-plane mode using 2-D incident wave spectra reconstructed from the NACCS parameters as offshore boundary conditions. STWAVE simulates wave propagation in the horizontal plane, including refraction based on geometric optic theory and shoaling based on the conservation of wave action along wave rays. Sea

Table 2 Nested coastal computational grid characteristics for wave simulations

Xo (UTM)	Yo (UTM)	α (°)	Discretization (m)	Length I direction (m)	Width J direction (m)	NI	NJ
284700	4576100	100	10	9900	12000	990	1200

Table 3 Nested coastal grid spectral characteristics and boundary conditions

Depth (m)	H_s (m)	T_p (s)	Offshore BC	Sides BC
35–42	7	20	TMA spectrum	Open water

state grows through the transfer of momentum from the wind field to the wave field, modeled using Resio's formulation (1981, 1987, 1988). Nonlinear energy transfer due to wave–wave interactions as first described by the Boltzmann integrals of Hasselmann et al. (1973) is implemented using Resio's methodology (Resio and Perrie 1991). The loss of energy by wave breaking is modeled using Miche's (1951) breaking criterion, which includes the effects of both water depth and wave steepness-limited breaking (Smith et al. 1997). The energy loss is simulated by reducing the spectral energy in each frequency and directional band proportionally to the amount of pre-breaking energy contained in each band. The bottom friction loss is implemented in this version of STWAVE (V6) using a Manning coefficient formulation (Holthuijsen 2007), which can be specified as a spatially variable parameter.

Two major simplifying assumptions were made for SLR scenarios. First, both storm surge and SLR are assumed to be uncoupled and thus are simply linearly superimposed. It was shown that a static model would tend to under-predict maximum water levels (Bilskie et al. 2014). Second, the NACCS 100-year storm spectral parameters are estimated using standard generalized extreme value statistics, based on the assumption of a steady-state system. We recognize that this assumption is violated since the system is transient. Both theoretical (e.g., Emanuel 1988; Holland 1997) and numerical (e.g., Bender and Ginis 2000) analyses predict a future intensification of extreme storms, as a result of the expected increase in sea surface temperature. Lin et al. (2012) showed that combining effects of storm climatology change and a 1 m SLR may cause the present NYC 100-year surge flooding to occur much more frequently, every 3–20 year. Lopeman et al. (2015) using state of the art statistical estimations, showed that storm Sandy (October, 2012) was a 108-year return period storm, which would correspond to a 28-year return period for a 1 m SLR. Based on these assumptions, the NACCS 100-year mean statistics are likely underestimating the future most likely 100-year water elevation. This potential underestimation of the predicted hazard, and consequently of the perceived risk, with the objective of protecting the coastal communities, led us to perform our simulations using the upper 95% confidence interval value for the projected 100-year static water level, which indeed increases the static water level by about 1.2 m, from about 2.5 to 3.7 m.

2.2 Pathway

Comparing the static water level expected for a 100-year storm (about 3.7 m) and the dune elevation of the barrier (about 3.5–4.2 m) shows that the Charlestown barrier island system should principally be in an overwash and inundation regime during a 100-year event, in view of the absence of significant dune volume above the still water elevation (Sallenger 2000). Most waves would impinge on or overtop the dunes, causing erosion and sediment transport, both landward (as washover fans) and offshore. This essentially flattens the profile and enhances subsequent wave propagation inside the coastal pond. This process is simulated in the storm scenarios by creating a realistic 100-*year dune profile,* which

replaces the current dune topography. This 100-year profile is an empirical topographic profile estimated based on the effects of the condition of the barriers following historic (1938 Hurricane and Hurricane Carol, 1954) storm events (Oakley 2016).

For long-term SLR scenarios, the erosion process is more complex since one would expect the dune to retreat landward over the years consistent with the beach equilibrium profile. The rate of dune retreat is semiempirically estimated based on local measurements and the beach equilibrium profile theory.

Boothroyd et al. (2016) calculated annualized shoreline change rates [1939–2014] along the Southern RI shore based on aerial imagery at transects spaced 50 m along the shoreline. Our study area, Charlestown RI, encompasses two geological/geomorphological zones, a barrier and the headland characterized by stratified glacial sediment, with corresponding average erosion rates, R_{do} and R_{ho}, of 0.57 m/year and 0.31 m/year, respectively (Fig. 2).

Local sea level data recorded at the Newport, RI NOAA tidal gage (1930–2006), yields an average SLR value, S_0, of 0.00258 m/year with a 95% confidence interval of ± 0.00019 m/year.

Assuming a linear relationship between erosion and SLR, following beach equilibrium profile theory, the dune recession rate, RR_i, for a specific geomorphologic entity (i), can be expressed in distance per meter of SLR as the ratio of erosion rate to SLR rate,

$$\mathrm{RR}_i = \frac{R_{i0}}{S_0} \tag{2}$$

with $i = d$ or h, for the dune and the headland rates, respectively. This results, for the Charlestown Barrier Island, in a recession rate, RR_d, on the order of 220 m per meter of SLR, and for the headland, the recession rate, RR_H, is 120 m per meter of SLR. Consequently the projected erosion distance normal to the shoreline, $\mathrm{R_i}$ (m) is a linear function of the projected SLR, S (m) given by,

$$R_i = \mathrm{RR}_i \times S \tag{3}$$

These recession rates are consistent with those found in the literature. Leatherman et al. (2000) have estimated empirically an average recession rate, RR, at the turn of the millennium, of 150 m/m for a sample of US East Coast beaches. Differences between headland and barrier recession rates are also consistent with Dean's theoretical approach which predicts a much faster recession rate for barriers (Dean and Dalrymple 2004).

It should be stressed that these retreat rates are empirical and therefore combine erosion due to SLR as well as erosion (or accretion) due to potential changes in storm intensity, duration, and frequency pattern. Therefore, erosion projections assume that the current storm pattern is steady state, as they rely on the observed linear relationship between sea level rise and erosion. This relationship is spatially dependent, since it is a function of coastal geology, geomorphology, and hydrodynamic processes specific to the study area of interest.

In the 100-year storm scenarios that assume SLR, the dune recesses according to Eq. (2) and rises to keep a similar elevation relative to MSL as the current dune. We have also simulated an alternative scenario, for which the rapid rate of SLR causes the dune to become submerged and drowned. There is indeed a certain threshold of SLR, depending upon the rate of sediment supply and the rate of SLR, where the dune might drown, either in-place (Sanders and Kumar 1975), or more likely, progressively, transgressing faster with decreased height and width and more frequent overwash events (Gutierrez et al. 2007).

2.3 Natural scenarios

We considered the 100-year storm risk occurring either today or in 2100. Two SLR scenarios were selected, 2 and 7 ft by 2100 (0. 60 and 2.1 m). For each SLR scenario, short term, long term, or both erosion processes were assumed, resulting in different dune profiles. These likely natural scenarios, for the 100-year storm pathway, are summarized in Table 4.

In Scenarios 1 and 2, the 100-year storm is assumed to occur in the very near future, when changes in sea level due to SLR are negligible. The only expected change in the coastline is at the scale of the storm event, the dune erosion due to the storm itself. Simulations are performed for an *intact dune* scenario (scenario 1) as well as for an *eroded dune* scenario (scenario 2), corresponding to likely initial and final stages of dune erosion if such a storm were to occur.

The hypothetical 100-year dune profile for the study area is shown in Fig. 3 (Oakley 2016). For scenario 2, this profile was substituted for the current dune topography to provide a hypothetical 100-year storm bathymetry/topography (digital elevation model) to be used in wave propagation simulations.

In Scenarios 3–6, a SLR of 2 ft (0.6 m) (scenarios 3 and 4) and 7 ft (2.1 m) (scenarios 5 and 6) were considered. These scenarios have an elevated water level and a modified shape of the shoreline. The MSL is moved up by the value of SLR, resulting in shoreline erosion. For each SLR scenario, two dune profile scenarios are simulated, depending on the ability of the dune system to keep up with SLR, progressively recessing and rebuilding. In scenarios 3 and 5, the dune retreats based on an empirical equilibrium slope parameter (γ) determined from historical erosion rates and measured SLR; in scenarios 4 and 6, the combination of SLR and increase in storm frequency evolves too fast to provide the necessary recovery time for the dune to rebuilt and retreat. The dune is thus overtopped by SLR and drowns.

The local bathymetry is modified for scenarios 2 through 6. In scenario 2, the 100-year storm dune profile is substituted for the current dune profile. In scenarios 3 and 5, the dune is recessed and raised according to the distance associated with the corresponding SLR, preserving its current projected 100-year storm profile. The beach on the headland is similarly recessed according to its erosion rate (Table 4). In scenarios 4 and 6, the headland beach is similarly recessed, but the dune is fully eroded. Waves simulations were performed with STWAVE for each coastline configuration and associated bathymetry.

2.4 Remediation scenarios

In addition to the above six *natural* scenarios, three hypothetical *remediation* scenarios were explored, to better assess the sensitivity of the risk to the storm pathway as well as to the resilience of the system: (1) The dune is sufficiently re-nourished such that the dune reservoir is sufficient to prevent the 100-year storm to overtop and erode the dune; (2) all houses in the flood inundated area are elevated to 9 ft (2.7 m) above the ground; and (3) both remediation scenarios (1) and (2) are combined. Each remediation scenario is applied to a 2-ft or 7-ft SLR scenario resulting in six remediation simulations summarized in Table 5.

Table 4 Simulated natural scenarios pathway's assumptions

Simulated natural scenarios						Historical data			Simulated coastline		
	Event scale	Long-term scale processes				Historical erosion rate (m/year)		Historical SLR (mm/year)	Projected dune recession (m) by 2100		100-year storm dune erosion
	Dune Erosion	SLR (m)	Headland Erosion	Dune Recession	Dune Fully Eroded	Headland (Glacial Till)	Dune (Dune Barrier)	Local rate (So)	Headland (RR_H)	Dune (RR_D)	
1	Intact	0									Intact
2	100-year profile	0									100-year profile
3	100-year profile	0.6	X	X		0.31	0.57	2.58	72	132	100-year profile [recessed]
4	Fully eroded	0.6	X		X	0.31	–	2.58	72		Fully eroded
5	100-year profile	2.1	X	X		0.31	0.57	2.58	252	462	100-year profile [recessed]
6	Fully eroded	2.1	X		X	0.31	–	2.58	252		Fully eroded

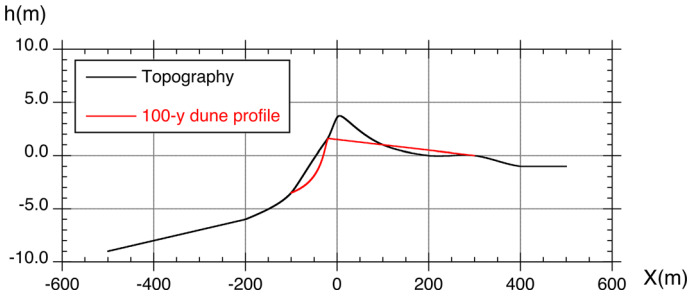

Fig. 3 Current dune cross-section (*black*) versus hypothetical 100-year storm dune profile (*red*). Cross-shore distance (x) versus dune elevation (h) (m; referred to NAVD88)

2.5 Risk

The risk is assessed in terms of expected residential damage calculated using the Coastal Environmental Risk Index (CERI; Spaulding et al. 2016). CERI uses damage curves developed by the USACE (Simm et al. 2015) to assess residential damage as a function of environmental hazard from storm surge and maximum wave elevation, and residential vulnerability. Inundation and wave damage are assessed separately. Vulnerability is defined for each individual house based on the value of four parameters: (1) number of floors, (2) presence or absence of a basement, (3) elevation of the first furnished floor (FFE), and (4) the house type (e.g., house on open piles, enclosed piles, no piles). The individual house's expected damage is a function of the structures parameter values, as well as environmental hazard quantified by the maximum inundation depth and critical wave crest height at the house. The risk associated with the 1% event is expressed in terms of the percentage of structural or content damage as a function of the water elevation/wave height (damage curve). For each hazard, surge and wave, each house type has three specific damage curves, *most likely, minimum,* and *maximum*, with the minimum to maximum reflecting other variables implicitly defining the resilience of the construction. House characteristics were obtained from the emergency call database (E911) as well as from independent surveys. For the sake of clarity and conciseness, results are presented for the maximum damage curve only (although all other results are available). Statistics are relative to the total number of houses in Charlestown RI in the 100-year storm inundation zone, including a SLR of 2.1 m (1323 residences).

3 Results

Results of each simulation are presented in the form of inundation maps (Figs. 4a, b, 5a, b, 6a, b, 7a, b), showing the total water depth (TWD), including surge and waves. TWD corresponds to FEMA's base flood elevation (BFE), however, referenced to ground level rather than to the standard vertical datum NAVD88. It combines storm surge, astronomical tide, wave setup, and the controlling wave crest, η_c in the flood inundated area following FEMA's terminology. The latter is defined as the mean of the 1% of the highest wave crests. Assuming that waves are Rayleigh distributed, $\eta_c = C_1 H_c$, with H_c the controlling wave height and $C_1 = 0.7$, and $H_c = C_2 H_s$, with H_s the significant wave height and $C_2 = 1.67$.

Table 5 Simulated remediation scenarios pathway and receptor resilience assumptions

Simulated remediation scenarios						Simulated coastline			Receptor resilience
	Event scale	Long-term scale processes				Projected dune recession (m) by 2100		100-year storm dune erosion	House remediation
	Dune erosion	SLR (m)	Headland erosion	Dune recession	Dune fully eroded	Headland (RR_{HL})	Dune (RR_D)		
7	INTACT-replenishment	0.6	X	X		72	132	Intact recessed	
8	100-year profile	0.6	X	X		72	132	100-year profile recessed	Houses elevated 9 ft above ground
9	INTACT-replenishment	0.6	X	X		72	132	Intact recessed	Houses elevated 9 ft above ground
10	INTACT-replenishment	2.1	X	X		252	462	Intact recessed	
11	100-year profile	2.1	X	X		252	462	100-year profile recessed	Houses elevated 9 ft above ground
12	INTACT-replenishment	2.1	X	X		252	462	Intact recessed	Houses elevated 9 ft above ground

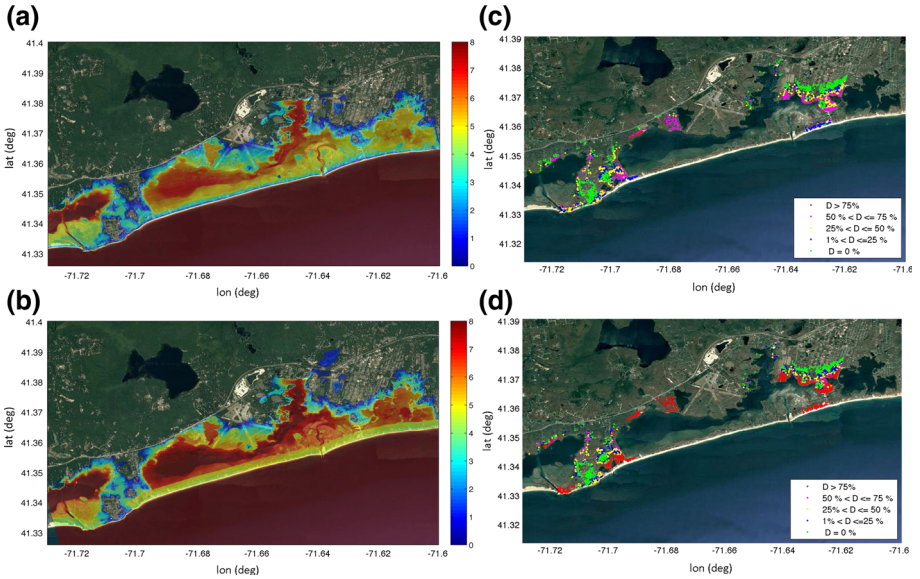

Fig. 4 Total water depth (TWD—m) for 100-year storm in Charlestown RI, for: **a** scenario 1 (no SLR, dune intact); and **b** scenario 2 (no SLR, dune eroded). Corresponding predicted damages are shown for each house in **c** and **d**, for scenarios 1 and 2, respectively (Spaulding et al. 2016)

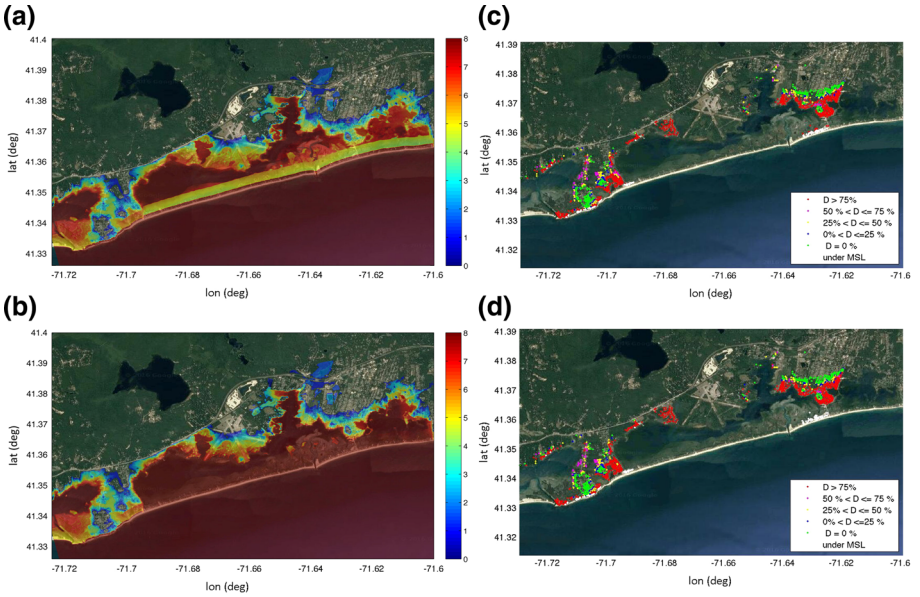

Fig. 5 Total water depth (TWD—m) for 100-year storm in Charlestown RI, for: **a** scenario 3 (2-ft SLR, dune raised); and **b** scenario 4 (2-ft SLR, dune flat). Corresponding predicted damages are shown for each house in **c** and **d**, for scenarios 3 and 4, respectively

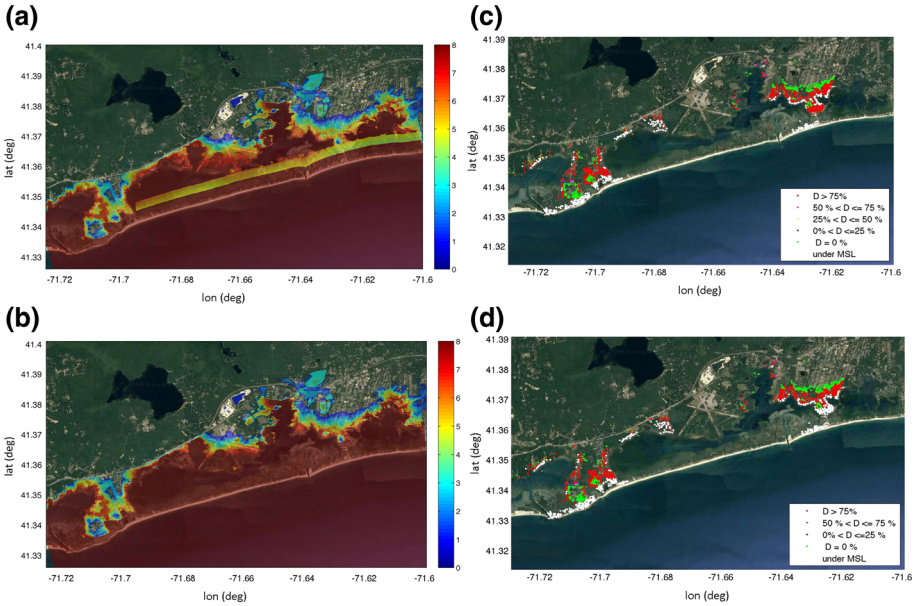

Fig. 6 Total water depth (TWD—m) for 100-year storm in Charlestown RI, for: **a** scenario 5 (7-ft SLR, dune raised); and **b** scenario 6 (7-ft SLR, dune flat). Corresponding predicted damages are shown for each house in **c** and **d**, for scenarios 5 and 6, respectively

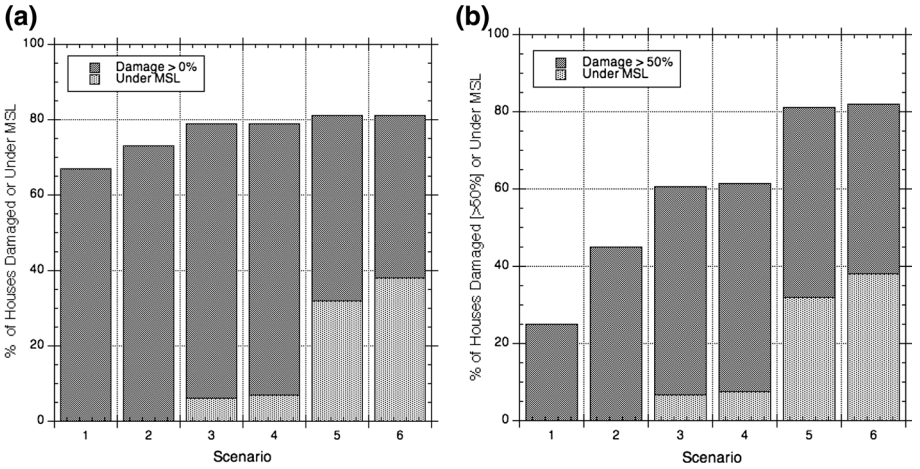

Fig. 7 Fraction (%) of the 1323 current houses in Charlestown, RI, damaged or under mean sea level (MSL), for six 100-year storm scenarios (Table 3). Damage refers to maximum structural damage. **a** Houses with damage larger than 0 and below MSL, and **b** represents houses with damage larger than 50% and below MSL

We mapped (Figs. 4c, d, 5c, d, 6c, d, 8) the corresponding maximum risk faced by individual houses, using as the risk proxy variable the maximum expected relative structural damage, with respect to the house value. Risk results are binned and color coded, such that houses with a predicted maximum relative structural damage between 0 and 25%, 25

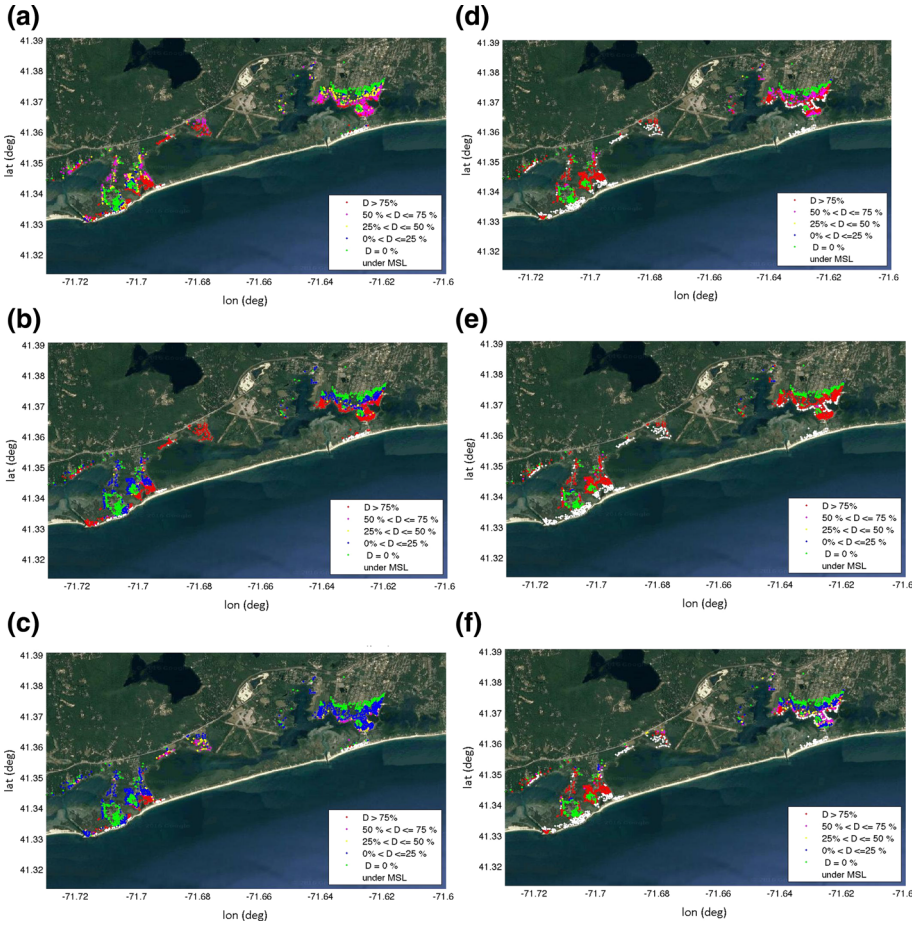

Fig. 8 Resulting damage for remediation scenarios: **a** 7; **b** 8; **c** 9, for a 2-ft SLR; **d** 10; **e** 11; and **f** 12, for a 7-ft SLR. The *upper maps* **a**, **d** assume a dune replenishment policy; the *middle maps* **b**, **e** assume an elevation of the houses to 9 ft; and *lower maps* **c**, **f** assume both remediation policies are implemented

and 50, 50 and 75%, and larger than 75%, are shown in each figure in blue, yellow, magenta and red, respectively. Houses in green have no predicted damage; houses shown in white would be under MSL in the scenarios with SLR, being either eroded or submerged. Table 6 shows the fraction of the 1323 current houses in Charlestown RI which would be damaged or under MSL for the six 100-year storm natural scenarios defined in Table 4, as well as for the four remediation scenarios (scenarios 7–10) defined in Table 5. Results are shown as the percentage of the houses with expected maximum structural damage larger than 0 or larger than 50% of the house value, as well as the fraction of houses under MSL. The 50% damage threshold is based on local coastal management rules that require buildings with damage greater than 50% to be rebuilt using the current building code. To facilitate the discussion in the following presentation, "high damage" will refer specifically to structural damage larger than 50% of the structural value and "high risk" will similarly refer to houses located in area expecting *high damage.*

Table 6 Results of simulations showing the fraction (%) of the 1323 houses potentially at risk in Charlestown RI damaged or under mean sea level (MSL) for six 100-year storm natural scenarios defined by sea level rise (SLR) and dune status as well as for the four remediation scenarios. Damage refers to the relative maximum structural damage (% house structural value)

Scenario	SLR (ft)	Dune status	Fraction of current houses damaged or under MSL (%)				Total damage >50% or under MSL
			Damage >0%	Damage >50%	Under MSL	Total damage >0 or under MSL	
1	0	Intact	67	25	0	67	25
2	0	Eroded 100y	73	45	0	73	45
3	2	Eroded 100y and recessed	73	54	6	79	60
4	2	Flatten	72	54	7	79	61
5	7	Eroded 100y and recessed	49	49	32	81	81
6	7	Flatten	44	44	38	82	82
7 Remediation #1 replenishment	2	Intact and recessed	72	45	6	79	51
8 Remediation #2 House 9 ft	2	Eroded 100y and recessed	71	38	6	77	44
9 Remediation #3 House 9 ft + replenishment	2	Intact and recessed	71	12	6	77	18
10 Remediation #1 replenishment	7	Intact and recessed	51	50	29	80	79
11 Remediation #2 House 9 ft	7	Eroded 100y and recessed	49	47	32	81	79
12 Remediation #3 House 9 ft + replenishment	7	Intact and recessed	51	32	29	80	61

Comparing scenario 1 and 2, we see that most of the houses would suffer little damage in current MSL conditions if the dune stayed intact (scenario 1), with only 25% of the houses showing high damage (Fig. 4a, c). However, if the dunes were eroded, being lowered and overtopped (scenario 2), the number of houses with high damage would be reaching 45%, resulting in an increase by 20% as compared to scenario 1 (Fig. 4b, d).

Under the assumption of 2-ft SLR, in scenario 3 (dunes recessed and raised), an additional 9% of the houses would suffer high damage relative to a similar scenario with no SLR (scenario 2) (Fig. 5a, c). Scenario 4 (dune drowned) does not predict an increase in estimated damage relative to scenario 3. Houses currently on the barrier beach would be fully eroded or under MSL according to both scenarios 3 and 4 (white dots in Fig. 5c, d) resulting in a total fraction of houses with high damage or under MSL of about 60%. Under the 7-ft SLR, similarly to the 2-ft SLR scenarios, damage is found to be very similar whether the dunes are recessed and raised (scenario 5; Fig. 6a, c) or drowned (scenario 6; Fig. 6b, d). Significantly more houses would be fully eroded and under MSL than in the 2-ft SLR cases (Fig. 6a,c) resulting in a total fraction of the houses with high damage or under MSL on the order of 80% (Table 5; Fig. 7).

Selected remediation scenarios for each SLR climate were explored to further assess the risk response to dune replenishment, as well as measures to elevate houses in low areas (Table 5). In scenarios 7 and 10, we propose beach replenishment, resulting in an hypothetical beach 100-year storm profile similar to the current beach profile, combined with a SLR scenario of 2 and 7 ft, for scenarios 7 and 10, respectively. In scenarios 8 and 11 we propose to elevate all houses to 9 ft above ground, combined with a SLR scenario of 2 and 7 ft, respectively. The 9-ft value is based on the average elevation of pile supported structures in the NACCS damage assessment study database (Simm et al. 2015). In scenarios 9 and 12, we combine both remediation scenarios, dune replenishment and house elevation, with a SLR scenario of 2 and 7 ft, respectively. Results are shown in the maps of Fig. 8 and summarized in Fig. 9.

Remediation simulations, however, show that each remediation policy indeed decreases the damage risk. These results are discussed in the next section.

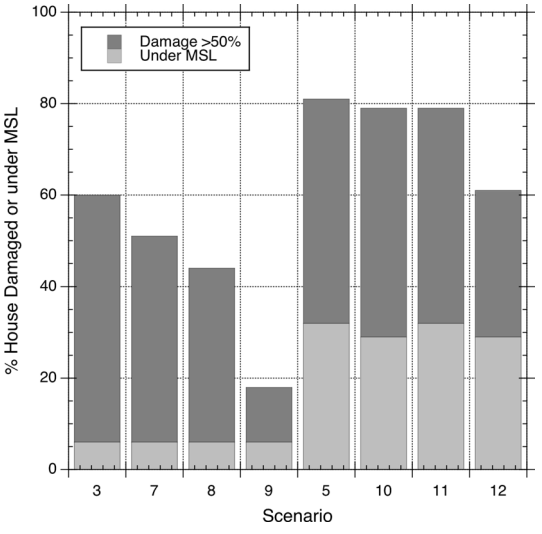

Fig. 9 Comparison of the relative fraction of houses with damage larger than 50%, as well as the relative fraction of houses under MSL for remediation scenarios 7–9 and 10–12 compared to SLR base case scenarios, 3 and 5, for SLR 2 ft and 7 ft, respectively

4 Discussion

Structural damage due to wave impact is strongly associated with the resilience of the dunes. Results of the simulations show that keeping the current dunes intact would significantly protect the Charlestown community against the 100-year storm. Most of the waves would break before reaching the dunes or at the dunes' toe, causing erosion, but not breaching the dunes. However, if the dunes were breached and overtopped as expected based on observations following historical storms, waves would propagate beyond the dune crest, across the pond, and would strongly impact houses on the landward edge of Ninigret Pond.

Under the assumption of SLR, besides damages due to the impact of the storm, a significant fraction of the current residences would be either eroded or under MSL by 2100, due to the change in the coastline morphology associated with SLR (dune recessed or drowned). In the 2-ft scenarios, about 7% of all houses in Charlestown, currently on the barrier beach would be fully eroded or under MSL according to both dune recessed or drowned scenarios (scenarios 3 and 4, respectively). For the 7-ft scenario this fraction would increase to 32–38% of the houses for both dune recessed or drowned scenarios (scenario 5 and 6, respectively). Let us note that this unexpected additional 6% of houses staying above MSL in scenario 5 (Fig. 6c) compared to scenario 6 (Fig. 6d) is an artifact of the design of the recessed dunes, which are retreating in a currently low area, thus elevating the latter to dune level and setting the houses at this location higher than they currently are. Therefore, assuming these houses are elevated, they might survive SLR based on this scenario's assumption; they, however, would risk suffering a 100% damage if the 100-year storm occurred (Fig. 6c).

Under the assumption of SLR, damage due to the 100-year storm would be increased compared to the non-SLR scenarios, but would be relatively similar whether the dunes are kept healthy (i.e., recessed and raised) or drowned. Indeed both cases allow for enough large waves to travel across Ninigret Pond to create major damage to the most exposed houses on the landward shore of the pond. When houses are exposed to waves, high damage is independent of wave height once these are above a certain threshold (order of 1 m of wave crest for non-elevated houses; NACCS 2015). Consequently by 2100, 60–80% of the current residences would be either eroded or experience damage larger than 50%, given a 2-ft or a 7-ft SLR scenario, respectively, assuming a similar 100-year storm and considering the change in the coastal morphology.

The current simulations do not predict any significant sensitivity to the dune crest elevation, as shown by comparing results of SLR simulations for the recessed and raised dunes with those of the fully drowned dunes. Indeed the 100-year storm surge is such that the SWEL is on the order of 4 m at the dune site, while the 100-year dune profile provides a dune crest eroded to 1.6 m (NAVD88). Therefore, in the 2-ft SLR case, the SWEL is about 3 m above the submerged dune crest, for the healthy dune, raised and recessed, scenario which, using Miche's breaking criteria in shallow water ($H_{max}/d = 0.88$; with d the water depth and H_{max} the maximum wave height), results in waves of about 2.6 m height (1.8 m wave crest) travelling across the pond. These waves are large enough to create high damage for most residence types. However, this insensitivity of the damage to the dune crest elevation for SLR scenarios is specific to the current 100-year design storm and to the local dune characteristics. For example, if we had used the mean storm surge value rather than its 95% confidence interval in the 100-year design storm, a healthy dune

raised and recessed would have provided a significantly stronger barrier against that storm than a drowned dune.

Remediation simulations show that each remediation policy indeed decreases the damage risk. When assuming a 2-ft SLR, dune replenishment would decrease the number of houses at high risk by 9% relative to scenario 3 (no remediation); elevating the houses would decrease this number by 16%; a combination of both remediation policies would dramatically decrease the number of houses at high risk by 42% relative to scenario 3, predicting only 12% of houses with damage larger than 50%.In case of a 7-ft SLR scenario, however, the success of such remediation scenarios is limited and a combination of both renourishment and structure elevation would provide a significant protection to about 17% of the current houses in Charlestown. In this case, we could expect a drop in number of houses at high risk from 49 to 32%.

The methodology presented here for Charlestown RI has been currently implemented for most of the RI coastline. It could easily be implemented in any other US coastal area where NACCS as well as shoreline erosion rate data are available. In areas where NACCS data are not available, extreme wave statistics and storm surge can be estimated from alternative sources such as WIS stations (waves), long-term buoy measurements, or NOAA large-scale storm surge simulations. Local erosion rates are based on empirical analyses of historic shoreline changes performed at a fine scale representative of the geological characteristics of the area combined with the scale of the relevant hydrodynamics processes (order of 50 m). However, as an alternative source of erosion data, CVDB provides a larger scale data set ($\sim$5 km resolution) for the US Atlantic, Pacific, and Gulf of Mexico Coasts (Hammar-Klose and Thieler 2001).

5 Conclusions

We have used a SPR approach to assess the risk of the coastal community of Charlestown, RI, to the 100-year storm, including effects of SLR and shoreline/dune erosion. Six *natural* storm scenarios were simulated, which were assumed to occur either in the near future, when SLR is negligible, or at the end of the century, when the expected SLR follows either a best-case scenario or a worst-case scenario, reaching 2 and 7 ft (0.6 and 2.1 m), respectively, by the end of the century. Additional *remediation* scenarios were simulated, in which we assumed that a dune replenishment program was implemented or a change in the resilience of the residences, achieved by elevating houses to 9 ft above grade.

Long-term shoreline erosion was simulated as a function of SLR, geology of the shoreline, and the year (time) of the simulated event, according to equilibrium beach profile theory, adjusted for empirical erosion rates and the SLR record. The topography and bathymetry in the study area were then modified accordingly for each inundation and wave propagation simulation. In addition, dune erosion at the scale of the storm event was included in the simulation by further modifying the topography and bathymetry to reflect the final dune profile, in overwash and inundation regime, a priori defined based on an empirical analysis of storm events and associated dune profiles. In cases with SLR an additional assumption is tested concerning the dune behavior, namely the total disappearance of the dune. For each scenario, we simulated nearshore wave propagation and coastal impact over a specified MSL including the effects of storm surge, tide and possible SLR, using the steady-state wave model STWAVE over a high-resolution (10-m) grid, input from the NACCS study, for both storm surge and wave energy spectra.

If no remediation measures are implemented for the Charlestown coastal community, the analysis predicts that, for a low SLR (2 ft) scenario, up to 54% of houses impacted would incur more than 50% of damage and 6% of the current houses would be permanently under MSL, resulting in 60% of the current houses being critically vulnerable. Assuming the high SLR (7-ft) scenario, up to about 30% of the current houses would be under MSL by the time the new MSL is reached. Approximately an additional 50% of the houses would suffer damage larger than 50% of their structural value, resulting in approximately 80% of the current residences being critically vulnerable.

Comparing results for the two possible natural behaviors for the dune system, either recession and rebuilding of the dune or total erosion and disappearance of the dune, we find approximately identical damage of the local residences; this is because the dune profile associated with the 100-year event would be so flattened than it would no longer significantly protect the community from offshore waves. At this stage, the only way to avoid storm damage is to have a sufficient base elevation, and only the houses that would be high enough in the topographical landscape would survive.

The remediation scenarios, i.e., replenishing the dune or creating a perched beach with an artificial submerged structure (artificial reef) to prevent the storm from overtopping the dunes, or elevating some houses, are all in principle very promising, especially when they are combined and one assumes a low SLR (2 ft) scenario. In this case, about 6% of the houses would still end up under MSL and be lost, but the fraction of houses suffering up to 50% damage would be reduced from 54% to 12% of the current houses in the community. About 550 houses currently exposed to high risk (more than 50% damage) in the 2-ft SLR scenario would be outside the high-risk areas if the combined remediation scenario would be implemented.

Under the assumption of a 7-ft SLR, the perspective is much more pessimistic since, even when combining the two remediation policies, 30% of the current houses would disappear as a result of SLR, ending up under the new MSL. The fraction of houses expecting possible damage larger than 50% would, however, be reduced by about 20%, from about 50–30%, compared to the situation without the remediation policies. This would remove about 260 houses from high-risk exposure.

This study demonstrates the importance of accurately predicting waves in storm events. The forces associated with large waves, in particular breaking waves, represent an additional hazard besides the storm surge, often ignored or simplified in hazard assessment. In addition, changes in the coastal geomorphology are shown to be critical in accurately defining the wave impact. In this analysis we show that under current MSL, waves associated to the 100-year storm increase the predicted fraction of houses with high damages in the Charlestown community by almost a factor 2, versus an assessment ignoring waves and the associated coastal erosion. Including SLR and the associated geomorphological changes in the shoreline increases the predicted fraction of houses with high damages by a factor 2.4–3.2 (2-ft or 7-ft SLR scenarios) compared to the no wave/no SLR scenario (25% of houses with high damage in scenario 1; 60–80% of houses with high damage in SLR scenarios).

We are aware that the method, as any deterministic modeling approach, carries a certain amount of uncertainty. At this stage we consider the method more as a resilience index than an exact damage predictor. We are currently working on developing a similar approach using alternative models to assess the epistemic uncertainty associated with the models selected and their assumptions. Results for remediation scenarios show that the fate of coastal communities sited at very low elevation strongly depends on marine and coastal policy. In order to communicate science effectively at the scale of the local community for

such sensitive issues, we believe that working toward improving model accuracy and quantifying uncertainty is of major importance.

Acknowledgements The authors gratefully acknowledge support for this work from the RI Coastal Resource Management Council. The application of the models to Charlestown, RI was supported by Housing and Urban Development (HUD), Grant #B-13-DS-44-0001 and administered through the State of Rhode Island, Executive Office of Commerce, Office of Housing and Community Development (OHCD). For providing the results of the NACCS study, we are indebted to Jane Smith, Mary Bryant Mary Cialone, Norberto Nadal-Carabello, and Jeff Melby of the US Army Corps of Engineers. We also thank the anonymous reviewers for their constructive comments.

References

Anderson ME, McKee-Smith J (2015) Implementation of wave dissipation by vegetation in STWAVE. ERDC/CHL CHETN-I-85, Vicksburg, MS: U.S. Army Engineering Research and Development Center

Bender MA, Ginis I (2000) Real-case simulations of hurricane-ocean interaction using a high-resolution coupled model: effects on hurricane intensity. Mon Weather Rev 128(4):917–946

Bender MA, Knutson TR, Tuleya RE, Sirutis JJ, Vecchi GA, Garner ST, Held IM (2010) Modeled impact of anthropogenic warming on the frequency of intense Atlantic hurricanes. Science 327(5964):454–458

Bilskie MV, Hagen SC, Medeiros SC, Passeri DL (2014) Dynamics of sea level rise and coastal flooding on a changing landscape. Geophys Res Lett 41:927–934

Bilskie MV, Hagen SC, Alizad K, Medeiros SC, Passeri DL, Needham HF, Cox A (2016) Dynamic simulation and numerical analysis of hurricane storm surge under sea level rise with geomorphologic changes along the northern Gulf of Mexico. Earth's Future 4(5):177–193

Boothroyd JC, Hollis RJ, Oakley BA, Henderson RE (2016) Shoreline change from 1939–2014, Washington County, Rhode Island. 1:2,000 scale. Rhode Island Geological Survey. 45 map

Bouws E, Günther H, Rosenthal W, Vincent CL (1985) Similarity of the wind wave spectrum in finite depth water: 1. Spectral form. J Geophys Res Oceans 90(C1):975–986

Bruun P (1962) Sea level rise as a cause of shore erosion. Am Soc Civil Eng Proc J Waterw Harb Div 88:117–130

Bruun P (1988) The Bruun rule of erosion by sea-level rise: a discussion on large-scale two- and three-dimensional usages. J Coast Res 4(4):627–648

Burzel A, Dassanayake DR, Oumeraci H (2015) Spatial modelling of tangible and intangible losses in integrated coastal flood risk analysis. Coastal Eng J 57(1):1540008

Church JA, White NJ (2006) A 20th century acceleration in global sea-level rise. Geophys Res Lett 33:L10602

Church JA, White NJ (2011) Sea-level rise from the late 19th to the early 21st century. Surv Geophys 32(4–5):585–602

Church JA, Clark PU, Cazenave A, Gregory JM, Jevrejeva S, Levermann A, Merrifield MA, Milne GA, Nerem RS, Nunn PD, Payne AJ, Pfeffer WT, Stammer D, Unnikrishnan AS (2013). Sea level change. In: Stocker TF, Qin D, Plattner G-K, Tignor M, Allen SK, Boschung J, Nauels A, Xia Y, Bex V, Midgley PM (eds) Climate change 2013: the physical science basis. Contribution of working group I to the fifth assessment report of the intergovernmental panel on climate change. Cambridge University Press, Cambridge

Cialone MA, Massey CT, Anderson ME, Grzegorzewski AS, Jensen RE, Cialone A, Mark DJ, Pevey KC, Gunkel BL, McAlpin TO, Nadal-Caraballo NN, Melby JA, Ratcliff JJ (2015) North Atlantic Coast Comprehensive Study (NACCS) coastal storm model simulations: waves and water levels. U.S. Army Engineer Research and Development Center, Technical Report. ERDC-CHL-TR-XX-draft

Cooper JAG, Pilkey OH (2004) Sea-level rise and shoreline retreat: time to abandon the Bruun Rule. Glob Planet Chang 43(3):157–171

Cui L, Ge Z, Yuan L, Zhang L (2015) Vulnerability assessment of the coastal wetlands in the Yangtze Estuary, China to sea-level rise. Estuar Coast Shelf Sci 156:42–51

Dean RG (1991) Equilibrium beach profiles: characteristics and applications. J Coast Res 7(1):53–84

Dean RG, Dalrymple RA (2004) Coastal processes with engineering applications. Cambridge University Press, Cambridge

Dean RG, Maurmeyer EM (1983) Models for beach profile response. In: Komar PD (ed) Handbook of coastal processes and erosion. CRC Press, Boca Raton, pp 151–166

Dietrich J, Zijlema M, Westerink J, Holthuijsen L, Dawson C, Luettich R, Jensen R, Smith J, Stelling G, Stone G (2011) Modeling hurricane waves and storm surge using integrally-coupled, scalable computations. Coast Eng 58:45–65

Emanuel K (1988) Toward a general theory of hurricanes. Am Sci 76:371–379
Emanuel KA (2013) Downscaling CMIP5 climate models shows increased tropical cyclone activity over the 21st century. Proc Natl Acad Sci 110(30):12219–12224
Emanuel K, Ravela S, Vivant E, Risi C (2006) A statistical deterministic approach to hurricane risk assessment. Bull Am Meteorol Soc 87:299–314
Emanuel K, Sundararajan R, Williams J (2008) Hurricanes and global warming: results from downscaling IPCC AR4 simulations. Bull Am Meteorol Soc 89:347–367
Godfrey PJ, Godfrey MM (1973) Comparison of ecological and geomorphic interactions between altered and unaltered barrier island systems in North Carolina. In: Coates DR (ed) Coastal Geomorphology. Publication in Geomorphology, State University of New York, pp 239–258
Gornitz V, Lebedeff S, Hansen J (1982) Global sea level trend in the past century. Science 215(4540):1611–1614
Grilli AR, Spaulding ML, Schambach L, Smith J, Bryant M (2015) Comparing inundation maps developed using WHAFIS and STWAVE. A case study in Washington County, Rhode Island. In: Proceedings of ASCE conference solutions to coastal disasters, Boston, MA (in process)
Gutierrez BT, Williams SJ, Thieler ER (2007) Potential for shoreline changes due to sea-level rise along the US Mid-Atlantic region. US Geological Survey
Gutierrez BT, Plant NG, Pendleton EA, Thieler ER (2014) Using a Bayesian network to predict shoreline change vulnerability to sea level rise for the coasts of the United States, Rep., 26 pp., U.S. Geol. Surv. Open-File Rep. 2014-1083
Hammar-Klose ES, Thieler ER (2001) Coastal vulnerability to sea level rise: a preliminary database for the U.S. Atlantic, Pacific, and Gulf of Mexico Coasts. U.S. Geological Survey, Digital Data Series DDS-68, 1 CD-ROM
Hasselmann K, Barnett TP, Bouws E, Carlson H, Cartwright DE, Enke K, Ewing JA, Gienapp H, Hasselmann DE, Kruseman P, Meerburg A, Muller P, Olbers DJ, Richter K, Sell W, Walden H (1973) Measurements of wind-wave growth and swell decay during the Joint North Sea Wave Project (JONSWAP). Deut Hydrogr Z Suppl A 8(12):1–95
Hay CC, Morrow E, Kopp RE, Mitrovica JX (2015) Probabilistic reanalysis of twentieth-century sea-level rise. Nature 517(7535):481–484
Holland GJ (1997) The maximum potential intensity of tropical cyclones. J Atmos Sci 54:2519–2541
Holman RA, Sallenger AH (1985) Setup and swash on a natural beach. J Geophys Res Oceans 90(C1):945–953
Holthuijsen LH (2007) Wave in ocean and coastal waters. Cambridge University Press, Cambridge, p 387
Horton BP, Rahmstorf S, Engelhart SE, Kemp AC (2014) Expert assessment of sea-level rise by AD 2100 and AD 2300. Quat Sci Rev 84:1–6
Hubert M, White K (2015) Sea-level change curve calculator. User Manual. U.S. Army Corps Of Engineers. Washington, DC
IPCC Fifth Assessment Report (AR5) (2014) https://www.ipcc.ch/report/ar5/
IPCC Fourth Assessment Report (AR4) (2007) IPCC Fifth. https://www.ipcc.ch/report/ar4/
Leatherman SP, Zhang K, Douglas BC (2000) Sea level rise shown to drive coastal erosion. Eos Trans Am Geophys Union 81(6):55–57
Levermann A, Clark PU, Marzeion B, Milne GA, Pollard D, Radic V, Robinson A (2013) The multimillennial sea-level commitment of global warming. Proc Natl Acad Sci 110(34):13745–13750
Lin N, Emanuel K (2016) Grey swan tropical cyclones. Nat Clim Change 6(1):106–111
Lin N, Emanuel K, Oppenheimer M, Vanmarcke E (2012) Physically based assessment of hurricane surge threat under climate change. Nat Clim Change 2:1–6
Lopeman M, Deodatis G, Franco G (2015) Extreme storm surge hazard estimation in lower Manhattan. Nat Hazards 78(1):355–391
Luettich RA Jr, Westerink JJ, Scheffner NW (1992) ADCIRC: an advanced three-dimensional circulation model for shelves coasts and estuaries, report 1: theory and methodology of ADCIRC-2DDI and ADCIRC-3DL, Dredging Research Program Technical Report DRP-92-6, U.S. Army Engineers Waterways Experiment Station, Vicksburg, MS, p 137
Massey TC, Anderson ME, McKee-Smith J, Gomez J, Rusty J (2011) STWAVE: steady state spectral wave model. User's manual for STWAVE, version 6.0
Medeiros S, Hagen S, Weishampel J, Angelo J (2015) Adjusting lidar-derived digital terrain models in coastal marshes based on estimated aboveground biomass density. Remote Sens 7(4):3507–3525
Miche M (1951) Le pouvoir reflechissant des ouvrages maritimes exposes a l'action de la houle. *Annals des Ponts et Chaussess*. 121e Annee: 285-319 (translated by Lincoln and Chevron, University of California, Berkeley, Wave Research Laboratory, Series 3, Issue 363, June 1954)

Moss RH, Edmonds JA, Hibbard KA, Manning MR, Rose SK, Van Vuuren DP, Carter TR, Emori S, Kainuma M, Kram T, Meehl GA (2010) The next generation of scenarios for climate change research and assessment. Nature 463(7282):747–756

NACCS (2015) North Atlantic comprehensive study: resilient adaptation to increasing risk. Physical Depth Damage Function. Summary report

Nadal-Caraballo NC, Melby JA, Gonzalez VM, Cox AT (2015) North Atlantic Coast Comprehensive Study (NACCS): coastal storm hazards from Virginia to Maine. U.S. Army Engineer Research and Development Center (ERDC), Technical Report. ERDC-CHL-TR-15-5

Narayan S, Simmonds D, Nicholls RJ, Clarke D (2015) A Bayesian network model for assessments of coastal inundation pathways and probabilities. J Flood Risk Manag. doi:10.1111/jfr3.12200

National Research Council (1987) Responding to changes in sea level. Engineering applications. National Academy Press, Washington

Naulin M, Kortenhaus A, Oumeraci H (2015) Reliability-based flood defense analysis in an integrated risk assessment. Coast Eng J 57(1):1540005

Nicholls RJ, Hanson SE, Lowe JA, Warrick RA, Lu X, Long AJ (2014) Sea-level scenarios for evaluating coastal impacts. WIREs Clim Change 2014(5):129–150

Oakley BA (2016) Generalized 1% storm barrier profile for the East Beach and Quonochontaug Barriers, Rhode Island: Technical report prepared for the Shoreline Change Special Area Management Plan

Orton PM, Hall TM, Talke SA, Blumberg AF, Georgas N, Vinogradov S (2016) A validated tropical-extratropical flood hazard assessment for New York Harbor. J Geophys Res Oceans 121(12):8904–8929

Oumeraci H (2004) Sustainable coastal flood defences: scientific and modelling challenges towards an integrated risk-based design concept. In: Proceedings of first IMA international conference flood risk assessment, University of Bath, UK, pp 9–24

Oumeraci H (2005) Integrated risk-based design and management of coastal flood defences. Die Küste 70:151–172

Oumeraci H, Kortenhaus A, Burzel A, Naulin M, Dassanayake DR, Jensen J, Wahl T, Mudersbach C, Gönnert G, Gerkensmeier B, Fröhle P (2015) XtremRisK—Integrated flood risk analysis for extreme storm surges at open coasts and in estuaries: methodology, key results and lessons learned. Coast Eng J 57(01):1540001

Parris A, Bromirski P, Burkett V, Cayan D, Culver M, Hall J, Horton R, Knuuti K, Moss R, Obeysekera J, Sallenger A, Weiss J (2012) Global sea level rise scenarios for the us National Climate Assessment. NOAA Tech Memo OAR CPO-1. p 37

Passeri DL, Hagen SC, Bilskie MV, Medeiros SC (2015) On the significance of incorporating shoreline changes for evaluating coastal hydrodynamics under sea level rise scenarios. Nat Hazards 75(2):1599–1617

Passeri DL, Hagen SC, Plant NG, Bilskie MV, Medeiros SC, Alizad K (2016) Tidal hydrodynamics under future sea level rise and coastal morphology in the Northern Gulf of Mexico. Earth's Future 4(5):159–176

Pendleton EA, Barras JA, Williams SJ, Twichell DC (2010) Coastal vulnerability assessment of the Northern Gulf of Mexico to sea-level rise and coastal change. US Department of the Interior, US Geological Survey

Peters GP, Andrew RM, Boden T, Canadell JG, Ciais P, Le Quéré C, Marland G, Raupach MR, Wilson C (2013) The challenge to keep global warming below 2 C. Nat Clim Change 3(1):4–6

Pfeffer WT, Harper JT, O'Neel S (2008) Kinematic constraints on glacier contributions to 21st-century sea-level rise. Science 321:1340–1343

Plant NG, Robert Thieler E, Passeri DL (2016) Coupling centennial-scale shoreline change to sea-level rise and coastal morphology in the Gulf of Mexico using a Bayesian network. Earth's Future 4(5):143–158

Reece JS, Passeri D, Ehrhart L, Hagen SC, Hays A, Long C, Noss RF, Bilskie M, Sanchez C, Schwoerer MV, Von Holle B (2013) Sea level rise, land use, and climate change influence the distribution of loggerhead turtle nests at the largest USA rookery (Melbourne Beach, Florida). Mar Ecol Prog Ser 493:259–274

Resio DT (1981) The estimation of wind-wave generation in a discrete spectral model. J Phys Oceanogr 11(4):510–525

Resio DT (1987) Shallow-water waves. I: theory. J Waterw Port Coast Ocean Eng 113(3):264–281

Resio DT (1988) Shallow-water waves. II: data comparisons. J Waterw Port Coast Ocean Eng ASCE. 114(1):50–65

Resio DT, Perrie W (1991) A numerical study of nonlinear energy fluxes due to wave-wave interactions Part 1. Methodology and basic results. J Fluid Mech 223:603–629. doi:10.1017/S002211209100157X

RIGIS (2013) Digital Elevation Model, DEM11. Rhode Island Geographic Information System (RIGIS) Data distribution System, http://www.edc.uri.edu/rigis. Environmental Data Center, University of Rhode Island, Kingston, Rhode Island (last date accessed 25 July 2013)

Rosati JD, Dean RG, Walton TL (2013) The modified Bruun Rule extended for landward transport. Mar Geol 340:71–81

Sallenger Jr AH (2000) Storm impact scale for barrier islands. J Coast Res 16(3):890–895

Sanders JE, Kumar N (1975) Evidence of shoreface retreat and in-place "drowning" during Holocene submergence of barriers, shelf off Fire Island, New York. Geol Soc Am Bull 86(1):65–76

Simm JD, Guise A, Robbins D, Engle J (2015) US North Atlantic coast comprehensive study: resilient adaptation to increasing risk. Coastal Management, 7–9 The Netherlands

Smith JM, Resio DT, Vincent CL (1997) Current-induced breaking at an idealized inlet. In: Proceedings of coastal dynamics'97. ASCE, pp. 993–1002

Smith JM, Sherlock AR, Resio DT (2001) STWAVE: Steady-state wave model user's manual for STWAVE, version 3.0. ERDC/CHL SR-01-01, Vicksburg, MS: U.S. Army Engineering Research and Development Center

Spaulding ML, Grilli A, Damon C, Crean T, Fugate G, Oakley BA, Stempel P (2016) STORMTOOLS: coastal environmental risk index (CERI). J Mar Sci Eng 4(3):54

Thieler ER, Hammar-Klose ES (2000) National assessment of coastal vulnerability to future sea-level rise: Preliminary results fort he U.S. Gulf of Mexico Coast

USACE (2011) Sea-level change considerations for civil works programs. Department Of The Army. U.S. Army Corps of Engineers. Washington, DC

Wamsley TV, Cialone MA, Smith JM, Ebersole BA, Grzegorzewski AS (2009) Influence of landscape restoration and degradation on storm surge and waves in southern Louisiana. Nat Hazards 51(1):207–224

Weyant J, Azar C, Kainuma M, Kejun J, Nakicenovic N, Shukla PR, La Rovere E, Yohe G (2009) Report of 2.6 versus 2.9 Watts/m^2 RCPP evaluation panel. Intergovernemental Panel on Climatic Change

Yan B, Li S, Wang J, Ge Z, Zhang L (2016) Socio-economic vulnerability of the megacity of Shanghai (China) to sea-level rise and associated storm surges. Reg Environ Change 16(5):1443–1456

Zervas C, Gill S, Sweet W (2013) Estimating vertical motion from long-term tide gauge records. Technical Report NOS CO-OPS 065. NOAA